

NANO EXPRESS

Open Access

Dielectric Relaxation of La-Doped Zirconia Caused by Annealing Ambient

CZ Zhao^{1,2*}, M Werner^{2,3}, S Taylor², PR Chalker³, AC Jones⁴, Chun Zhao^{1,2}

Abstract

La-doped zirconia films, deposited by ALD at 300°C, were found to be amorphous with dielectric constants (*k*-values) up to 19. A tetragonal or cubic phase was induced by post-deposition annealing (PDA) at 900°C in both nitrogen and air. Higher *k*-values (~32) were measured following PDA in air, but not after PDA in nitrogen. However, a significant dielectric relaxation was observed in the air-annealed film, and this is attributed to the formation of nano-crystallites. The relaxation behavior was modeled using the Curie–von Schweidler (CS) and Havriliak–Negami (HN) relationships. The *k*-value of the as-deposited films clearly shows a mixed CS and HN dependence on frequency. The CS dependence vanished after annealing in air, while the HN dependence disappeared after annealing in nitrogen.

Introduction

Amorphous ZrO₂ is one of the most promising dielectrics (dielectric constant *k*-value ~20) to replace SiO₂ in MOSFETs at the 45-nm node CMOS technologies. Due to the aggressive down-scaling of MOSFET, higher dielectric constant materials and higher mobility semiconductors other than silicon are introduced [1-11]. Germanium is considered to be a good candidate to replace silicon in the channel of next-generation high-performance CMOS devices, while rare earth oxides belonging to another class of materials offer good passivation of germanium to reduce the density of interface states, as it has recently been suggested [5,7,10]. On the other hand, theoretical studies have reported that the metastable tetragonal and cubic phases (*t*- and *c*-phases) of ZrO₂ have higher *k*-values [12,13]. The addition of rare earth elements, such as La, Gd, Dy, or Er, is reported to stabilize these phases and *k*-values of up to 40 have been obtained [7-11,14].

In order to induce the *t*- and *c*-phases in the La-doped ZrO₂, dielectric post-deposition annealing (PDA) is needed, otherwise the layers grown by atomic layer deposition (ALD) at relatively low temperatures (<450°C) have an amorphous microstructure [15,16]. However, the transformation from amorphous to *t*- and

c-phases can cause both dielectric relaxation and an adverse increase in the leakage current [14,17]. Leakage, which is the quantity defined in the ITRS Roadmap, depends on the combination of *k*-value and energy offset values between the energy bands of the high-*k* material and the silicon crystal. For example, 1×10^{-8} A/cm² is a value required for DRAM capacitors [18] (much higher values are accepted for gate oxides in CMOS). Since the purpose to introduce high-*k* dielectrics is to reduce the leakage current of gate oxides, a lot of investigations on the leakage current of high-*k* dielectrics have been carried out [19-23].

However, there is little information about dielectric relaxation of La-doped ZrO₂ dielectrics. Since loss due to the dielectric relaxation can cause MOSFET deterioration, the aim in this study was therefore to investigate the effect of PDA on the relaxation behavior of La-doped ZrO₂. In this paper, we report the influence of the annealing ambient on the dielectric relaxation processes, which can be described by both the Havriliak–Negami (HN) and Curie–von Schweidler (CS) relationships [24-27] in the frequency range of 10 MHz.

Experimental

La-doped ZrO₂ films, with a thickness of 35 nm, were deposited on n-type Si(100) substrates by liquid injection ALD at 300°C, using a modified Aixtron AIX 200FE AVD reactor configured for liquid injection [28]. Both Zr and La sources are Cp-based precursors

* Correspondence: cezhou.zhao@xjtlu.edu.cn

¹Department of Electrical and Electronic Engineering, Xi'an Jiaotong, Liverpool University, 215123, Suzhou, Jiangsu China.

Full list of author information is available at the end of the article

$[(\text{MeCp})_2\text{ZrMe}(\text{OMe})]$ and $[(\text{PrCp})_3\text{La}]$ [15,16]. The composition of the La-doped ZrO_2 films was estimated to be $\text{La}_{0.35}\text{Zr}_{0.65}\text{O}_2$ from Auger electron spectroscopy (AES). Selected films were annealed at 700°C or 900°C for 15 min, in an N_2 or air ambient.

The effects of PDA on the physical and electrical properties of the $\text{La}_{0.35}\text{Zr}_{0.65}\text{O}_2$ films have been investigated using cross-section transmission electron microscopy (XTEM), X-ray diffraction (XRD), high–low frequency capacitance–voltage (C–V), capacitance–frequency (C–f), and current–voltage (I–V) measurements, respectively.

In order to perform the C–V, C–f and I–V measurements, metal (Au) gate electrodes were evaporated to form metal–oxide–semiconductor capacitors (Au/ $\text{La}_{0.35}\text{Zr}_{0.65}\text{O}_2$ /IL/n-Si, where IL stands for interfacial layer) with an effective contact area of $4.9 \times 10^{-4} \text{ cm}^2$. The backside of the Si wafer was cleaned with a buffered HF solution, and subsequently a 200-nm-thick film of Al was deposited to form an ohmic back contact. A thermal SiO_2 sample was grown using dry oxidation at 1100°C to provide a comparison with the high-k stacks. Its back-side contact was prepared in exactly the same way as for all other $\text{La}_{0.35}\text{Zr}_{0.65}\text{O}_2$ samples: depositing Al after HF treatment.

Results and Discussion

XRD was carried out using a Rigaku Miniflex X-ray diffractometer with nickel-filtered $\text{Cu K}\alpha$ radiation ($\lambda = 1.5405 \text{ \AA}$) and a 2θ increment of 0.2° per minute, and the results are shown in Figure 1. Results from the

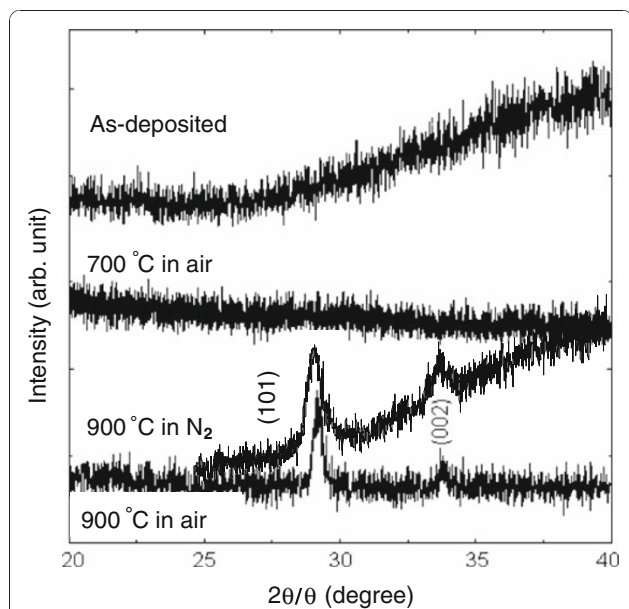


Figure 1 X-ray diffraction data for $\text{La}_{0.35}\text{Zr}_{0.65}\text{O}_2$ films deposited by ALD and then annealed in air or N_2 for 15 min at different temperatures.

as-deposited samples and samples annealed at 700°C showed that the films were amorphous. XRD spectra from both samples annealed at 900°C show two clear diffraction peaks at 29.3° and 33.9° , suggesting that crystallization starts between 700 and 900°C . These peaks correspond to the t- or c- phases, but it is difficult to distinguish between them. Selected area diffraction results (not shown) obtained using a TEM would suggest that the cubic phase is the most likely.

XTEM was carried out on both the 900°C PDA samples using a JEOL 2000FX operated at 200 kV. XTEM images in Figure 2 show that equiaxed nano-crystallites of $\sim 4 \text{ nm}$ diameter were formed in the air-annealed sample, in comparison with larger $\sim 15\text{-nm}$ crystals for the N_2 -annealed sample. The thickness of the $\text{La}_{0.35}\text{Zr}_{0.65}\text{O}_2$ layers and the IL was also obtained by XTEM. The 35-nm-thick $\text{La}_{0.35}\text{Zr}_{0.65}\text{O}_2$ layers retained their thickness after PDA, but the IL increased from 1.5 nm on the as-deposited samples to 4.5 nm and 6 nm after PDA at 900°C in N_2 and in air, respectively, which is attributed to either an internal or external oxidation mechanism. Previous medium energy ion scattering (MEIS) results [16] showed the incorporation of some La in the IL, which is reported to increase the k-value of the IL from 3.9 (pure SiO_2) to ~ 10 [29].

C–V and C–f measurements were carried out using a HP4192 impedance analyzer and an Agilent E4980A LCR meter at various frequencies (20 Hz–13 MHz) in parallel mode. C–f measurements were performed at a strong accumulation region ($V_g = +3 \text{ V}$). C–V measurements were carried out from strong inversion toward strong accumulation and vice versa. Three typical sets of C–V curves of the as-deposited and PDA samples were shown in Figure 3. PDA was found to

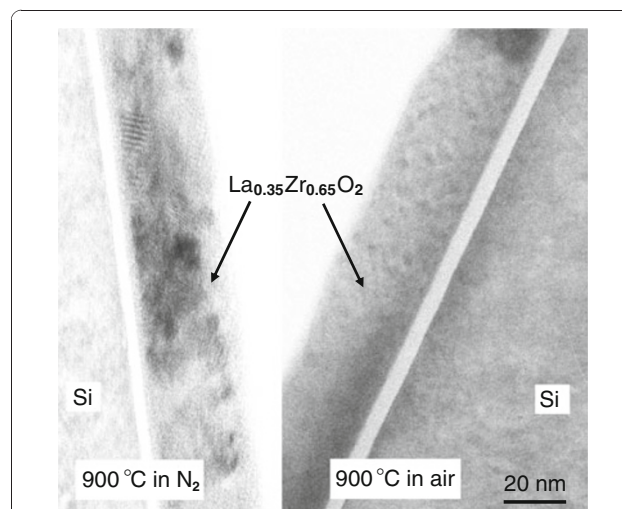


Figure 2 XTEM images from $\text{La}_{0.35}\text{Zr}_{0.65}\text{O}_2$ samples, which were annealed in air and N_2 at 900°C for 15 min, respectively.

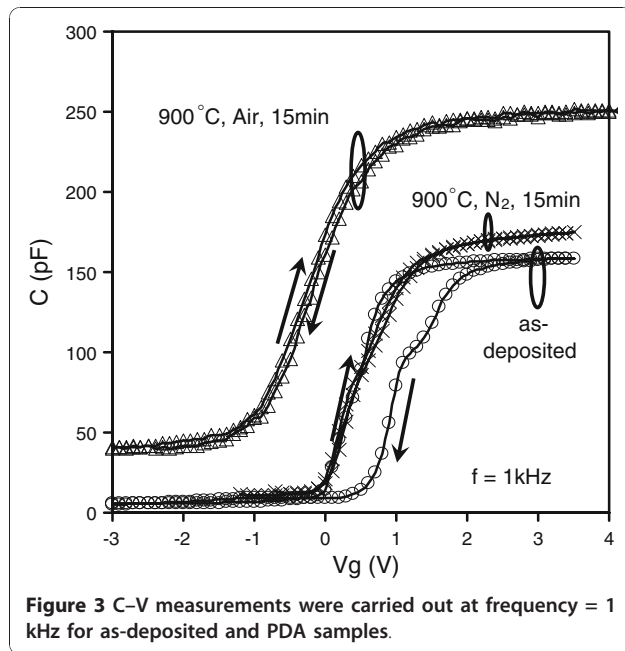


Figure 3 C–V measurements were carried out at frequency = 1 kHz for as-deposited and PDA samples.

significantly reduce the hysteresis to ~ 10 mV (counter-clockwise), independent of the annealing ambient. PDA in air caused a negative shift of the C–V curves due to positive charge generation and also caused an enhanced accumulation capacitance, which originated from a k -value increase in the $\text{La}_{0.35}\text{Zr}_{0.65}\text{O}_2$ layer. Positive charge generation will be discussed first, and then the k -value increase.

From the early days of silicon technology, thermal oxidation of Si has been known to introduce fixed positive charge at the Si/SiO₂ interface [30]. Positive charge generation during high-temperature processing is not new to thin film SiO₂ physics; its presence has been detected ever since the pioneering era of Si oxidation in the form of fixed oxide charge that often develops during the oxidation process [31]. The presence of positively charged, over-coordinated oxygen centers in SiO₂ has been suggested previously in the work of Snyder and Fowler [32]. They showed that the positive charge involved with the E' oxygen-vacancy center is in fact associated with over-coordination of an O. Warren et al. suggested that the formation of positively charged over-coordinated O defects is near the Si/SiO₂ interface [33,34]. The effect of post-deposition oxidation of SiO_x/ZrO₂ gate dielectric stacks at different temperatures (500–700°C) on the density of fixed charge was proposed by Houssa et al. [35]. They indicated that increasing oxidation temperature, the density of negative fixed charge is reduced. The net positive charge observed after oxidation at $>500^\circ\text{C}$ resembles the charge generated at the Si/SiO₂ interface by hydrogen in the same temperatures range. They

proposed that the observed oxidation-induced positive charge in the SiO_x/ZrO₂ gate stack may be related to over-coordinated oxygen centers induced by hydrogen. This also matches our previous observations at the Si/SiO₂ and Si/SiO₂/HfO₂ structures [36,37].

Before discussing the k -value increase, the causes of frequency dispersion must be totally understood. Figure 4 (a) indicates that a large frequency dispersion was observed during C–V measurements in the air-annealed sample. There are five reasons that may cause the frequency dispersion observed: (1) series resistances, (2) parasitic effects (including back contact imperfection and cables and connections), (3) leakage currents, (4) the interlayer between $\text{La}_{0.35}\text{Zr}_{0.65}\text{O}_2$ layer and semiconductor silicon substrate, or (5) a k -value dependence on frequency of the $\text{La}_{0.35}\text{Zr}_{0.65}\text{O}_2$ dielectric. To obtain the genuine intrinsic properties and permittivity of the $\text{La}_{0.35}\text{Zr}_{0.65}\text{O}_2$ dielectric from the CV measurements, the first four effects must be eliminated.

The effects of series resistances and parasitic effects were reported in our previous work [38]. To minimize the effects of series resistances and back contact imperfections (including contact resistance R , contact capacitance C , or parasitic R–C coupled in series, etc.), aluminum back contacts were deposited over a large area of the substrate wafer that was cleaned with a buffered HF solution before aluminum contacts were formed. The same procedure was carried out for all as-deposited, N₂-annealed, and air-annealed samples. All samples tested had the same or very similar substrate area ($\sim 2 \times 2$ cm²) to ensure that the effects of series resistance and back contact imperfections were the same for all samples. Furthermore, measurement cables and connections were kept short to further minimize parasitic capacitance effects and were the same for all samples. To provide a comparison with Figure 4a, a C–V measurement on a thermal SiO₂ sample with the same HF treatment and Al deposition on its back was carried out from the same test system; the results are shown in Figure 4b. It is clear that no frequency dispersion was observed on the thermal SiO₂ sample. Therefore, the effects of series resistances and parasitic effects are negligible.

The leakage current characteristics of the La-doped films were evaluated from the I–V measurements, as shown in Figure 5. At low oxide fields (E_{ox} at 0 to +2MV/cm), the leakage current density is improved under positive gate biases after annealing, which is attributed to the thicker IL. However, PDA also causes crystallization that introduces leakage current paths and reduces the break-down voltage. The leakage current densities at +2MV/cm are 1.6×10^{-5} Acm⁻² for as-deposited samples, but below 5×10^{-8} Acm⁻² after the 900°C PDA either in N₂ or in air. This suggests that the

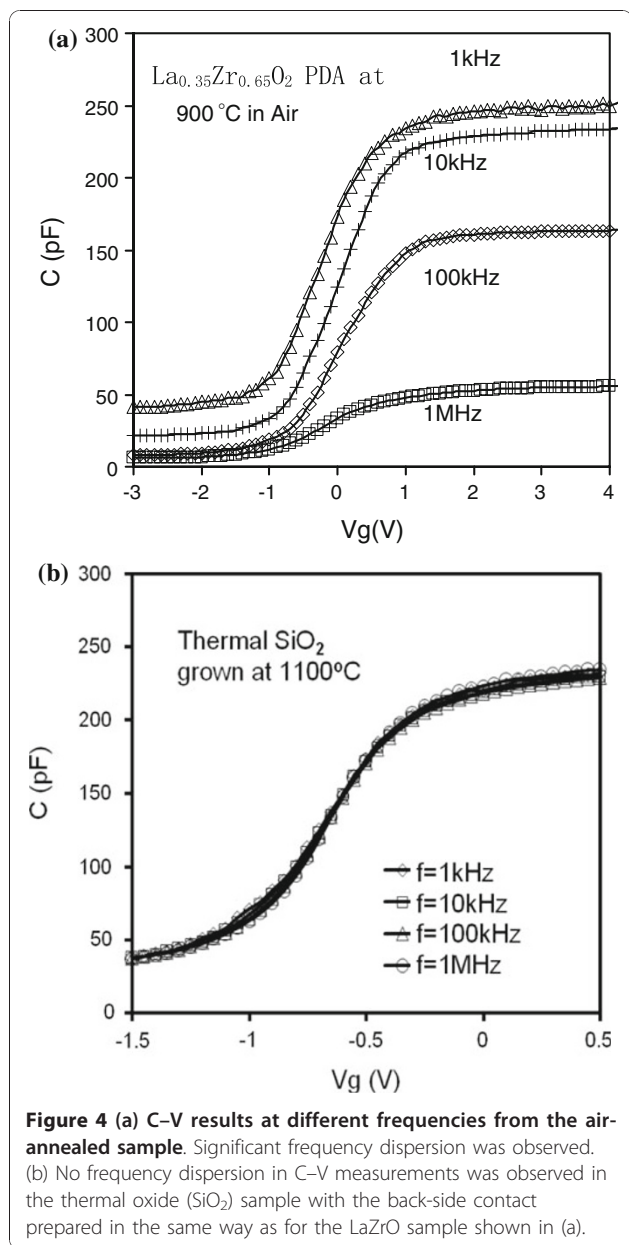


Figure 4 (a) C-V results at different frequencies from the air-annealed sample. Significant frequency dispersion was observed. (b) No frequency dispersion in C-V measurements was observed in the thermal oxide (SiO₂) sample with the back-side contact prepared in the same way as for the LaZrO sample shown in (a).

effect of leakage currents on frequency dispersion is negligible during C-V measurements.

Before k-value of the La_{0.35}Zr_{0.65}O₂ dielectric is extracted from the strong accumulation capacitance at +3 V (<+1MV/cm), the effect of the presence of the lossy interlayer must be taken into account. The effect was also reported in our previous work [38].

The relationship between the extracted k-value and test frequency shown in Figure 6 indicates that significant dielectric relaxation only occurs in the air-annealed sample. Parasitic effects could not be the cause of the frequency dispersion observed because of the sample preparation and measurement procedures described

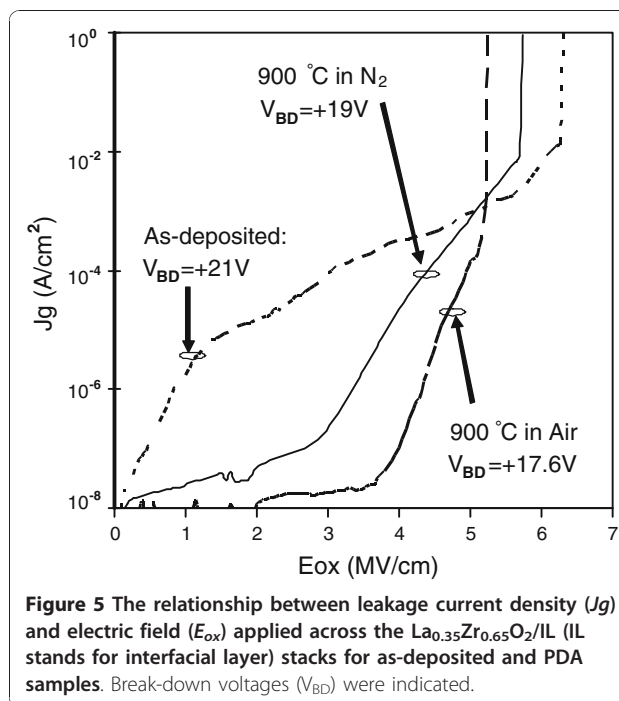


Figure 5 The relationship between leakage current density (J_g) and electric field (E_{ox}) applied across the La_{0.35}Zr_{0.65}O₂/IL (IL stands for interfacial layer) stacks for as-deposited and PDA samples. Break-down voltages (V_{BD}) were indicated.

earlier. Significant frequency dispersion was not seen in other MOSCs fabricated using the same substrates prepared and measured in exactly the same way. We conclude therefore that the frequency dispersion observed in the La_{0.35}Zr_{0.65}O₂ film annealed in air is a real material property of this dielectric. There are two important observations in Figure 6: (1) PDA in air increases the

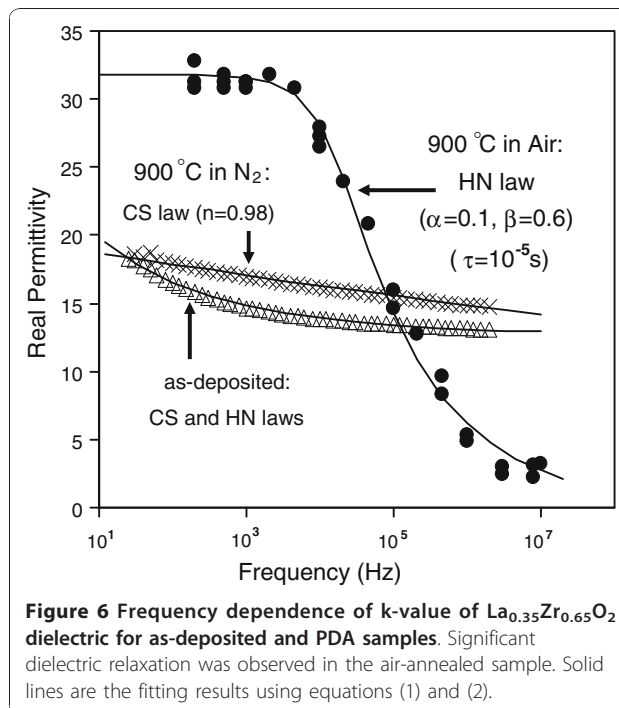


Figure 6 Frequency dependence of k-value of La_{0.35}Zr_{0.65}O₂ dielectric for as-deposited and PDA samples. Significant dielectric relaxation was observed in the air-annealed sample. Solid lines are the fitting results using equations (1) and (2).

k-value of the $\text{La}_{0.35}\text{Zr}_{0.65}\text{O}_2$ dielectric significantly (k -value reaches 32 at 1 kHz), along with a significant dielectric relaxation. (2) There is less of an effect on the k -value for the film annealed in N_2 , with a small increase in k -value at some frequencies and a flatter frequency response compared to the as-deposited sample. Both effects of temperature/ambient and causes of dielectric relaxation are discussed later.

Annealing at a high temperature is employed to induce the t- and c-phases in the La-doped ZrO_2 dielectric from the amorphous samples [15,16]. The addition of La is to stabilize these phases, and the stabilized tetragonal/cubic ZrO_2 phase gives a higher k -value [7-14]. Annealing temperature was reported to range from 400 to 1,050°C, depending on the deposition conditions and substrates of high- k dielectrics that determine the microstructure of the as-deposited samples. It was reported that the germanium substrate requires lower annealing temperatures ranging from 400 to 600°C [7-11]. If the microstructure of the as-deposited LaZrO_2 samples had already been tetragonal/cubic, annealing at high temperatures would not be necessary [9].

It has been shown previously that dielectric relaxation in the time domain can be described by a power-law time dependence, t^{-n} [26,27], or a stretched exponential time dependence, $\exp[-(t/t_0)^m]$ [39,40], where n and m are parameters ranging between 0 and 1, and t_0 is a characteristic relaxation time.

In the frequency domain, after a Fourier transform, the corresponding dielectric response of t^{-n} dependence is well described in terms of Curie–von Schweidler (CS) behavior [24,26,27], while the Fourier transform of $\exp[-(t/t_0)^m]$ function into frequency domain can be approximated by a Havriliak–Negami (HN) relationship [25], after a great deal of work [41-43]. The CS law and HN relationship can be, respectively, expressed as

$$\varepsilon_{CS}(\omega) - \varepsilon_{\infty} = A(i\omega)^{n-1} \quad (1)$$

$$\varepsilon_{HN}(\omega) - \varepsilon_{\infty} = (\varepsilon_s - \varepsilon_{\infty}) / \left[1 + (i\omega\tau)^{1-\alpha} \right]^{\beta} \quad (2)$$

where ε_s and ε_{∞} are the static and high-frequency limit permittivities, respectively; τ is the HN relaxation time; $\omega = 2\pi f$ is the angular frequency; and n , α , and β are the relaxation parameters.

A theoretical description of the slow relaxation in complex condensed systems is still a topic of active research despite the great effort made in recent years. There exist two alternative approaches to the interpretation of dielectric relaxation: the parallel and series models [44]. The parallel model represents the classical relaxation of a large assembly of individual relaxing

entities such as dipoles, each of which relaxes with an exponential probability in time but has a different relaxation time t_k . The total relaxation process corresponds to a summation over the available modes k , given a frequency domain response function, which can be approximated by the HN relationship.

The alternative approach is the series model, which can be used to describe briefly the origins of the CS law (the t^{-n} behavior). Consider a system divided into two interacting sub-systems [45]. The first of these responds rapidly to a stimulus generating a change in the interaction which, in turn, causes a much slower response of the second sub-system. The state of the total system then corresponds to the excited first system together with the unresponded second system and can be considered as a transient or metastable state, which slowly decays as the second system responds.

In some complex condensed systems, neither the pure parallel nor the pure series approach is accepted and instead interpolates smoothly between these extremes [46]. The CS behavior has to be faster than the HN function at short times and slower than the HN function at long times.

Based on the discussion above, the dielectric relaxation results (shown in Figure 6) have been modeled with the CS and/or HN relationships (see solid lines in Figure 6). The relaxation of the as-deposited film obeyed a mixed CS and HN relationships. After the 900°C PDA, the relaxation behavior of the N_2 -annealed film was dominated by the CS law, whereas the air-annealed film was predominantly modeled by the HN relationship that was accompanied by a sharp drop in the k -value.

Although the exact microstructural cause of these relaxation processes is not clearly known, several mechanisms for the dielectric relaxation have been proposed, including distribution of relaxation time [47], distribution of hopping probabilities [48], space charge trapping [49], self-similar multi-well potential for ionic configurations [45], or double potential well occupied by one electron [50]. However, it has been reported that a decrease in crystal grain size can cause an increase in the dielectric relaxation in ferroelectric relaxor ceramics [51,52]. This relaxation effect has been attributed to higher stresses in the smaller grains [51]. A similar effect appears to have occurred with these La-doped dielectric films, with the 900°C air anneal producing 4-nm diameter equiaxed nano-crystallites within the film, and suffering from a severe dielectric relaxation. The 900°C N_2 -annealed film contains much larger ~15-nm crystals and does not suffer from severe dielectric relaxation. Therefore, the physical processes behind the relaxation are probably related to the size of the crystal grains formed during annealing.

Conclusions

PDA at 900°C either in N₂ or in air causes crystallization (t- or c-phases) of the La_{0.35}Zr_{0.65}O₂ dielectric. Larger crystal grain sizes were observed in the N₂-annealed sample than in the air-annealed sample. Following PDA in N₂, the k-value was maintained and the dielectric relaxation was reduced. However, PDA in air causes a significant increase in k-value (32 at 1 kHz) and a significant dielectric relaxation, probably associated with smaller crystal grain sizes. The relaxation behavior of the as-deposited sample can be modeled using the mixed CS and HN relationships. PDA in N₂ suppressed the HN law, while the CS law was removed following PDA in air.

Acknowledgements

This research was funded in part from the Engineering and Physical Science Research Council of UK under the grant EP/D068606/1, the National Natural and Science Foundation of China under the grant no. 60976075, and the Suzhou Science and Technology Bureau of China under the grant SYG201007.

Author details

¹Department of Electrical and Electronic Engineering, Xi'an Jiaotong, Liverpool University, 215123, Suzhou, Jiangsu China. ²Department of Electrical Engineering and Electronics, University of Liverpool, Liverpool, L69 3GJ, UK. ³Department of Engineering, Materials Science and Engineering, University of Liverpool, Liverpool, L69 3GH, UK. ⁴Department of Chemistry, University of Liverpool, Liverpool, L69 3ZD, UK.

Received: 13 April 2010 Accepted: 9 September 2010

Published: 30 September 2010

References

1. Boscke TS, Govindarajan S, Fachmann C, Heitmann J, Avellan A, Schroder U, Kirsch PD, Krug C, Hung PY, Song SC, Ju BS, Price J, Pant G, Gnade BE, Krautschneider W, Lee B-H, Jammy R: *Tech Dig Int Electron Devices Meet* 2006, **255**.
2. Lu N, Li H-J, Peterson JJ, Kwong DL: *Appl Phys Lett* 2007, **90**:082911.
3. Darmawan P, Lee PS, Setiawan Y, Ma J, Oscipowicz T: *Appl Phys Lett* 2007, **91**:092903.
4. Lopes JMJ, Littmark U, Roeckerath M, St Lenk, Schubert J, Mantl S, Besmehn A: *J Appl Phys* 2007, **101**:104109.
5. Mavrou G, Galata S, Tsiapas P, Sotiropoulos A, Panayiotatos Y, Dimoulas A, Evangelou EK, Seo JW, Dieker Ch: *J Appl Phys* 2008, **103**:014506.
6. Abermann S, Bethge O, Henkel C, Bertagnolli E: *Appl Phys Lett* 2009, **94**:262904.
7. Abermann S, Henkel C, Bethge O, Pozzovivo G, Klang P, Bertagnolli E: *Applied Surface Science* 2010, **256**:5031.
8. Mavrou G, Tsiapas P, Sotiropoulos A, Galata S, Panayiotatos Y, Dimoulas A, Marchiori C, Fompeyrine J: *Appl Phys Lett* 2008, **93**:212904.
9. Tsoutsou D, Apostolopoulos G, Galata S, Tsiapas P, Sotiropoulos A, Mavrou G, Panayiotatos Y, Dimoulas A: *Microelectron Eng* 2009, **86**:1626.
10. Tsoutsou D, Lamagna L, Volkos SN, Molle A, Baldovino S, Schamm S, Coulon PE, Fanciulli M: *Appl Phys Lett* 2009, **94**:053504.
11. Lamagna L, Wiemer C, Baldovino S, Molle A, Perego M, Schamm-Chardon S, Coulon PE, Fanciulli M: *Appl Phys Lett* 2009, **95**:122902.
12. Vanderbilt D, Zhao X, Ceresoli D: *Thin Solid Films* 2005, **486**:125.
13. Zhao X, Vanderbilt D: *Phys Rev B* 2002, **65**:233106.
14. Govindarajan S, Boscke TS, Sivasubramani P, Kirsch PD, Lee BH, Tseng H-H, Jammy R, Schroder U, Ramanathan S, Gnade BE: *Appl Phys Lett* 2007, **91**:062906.
15. Gaskell JM, Jones AC, Aspinall HC, Taylor S, Taechakumput P, Chalker PR, Heys PN, Odedra R: *Appl Phys Lett* 2007, **91**:112912.
16. Gaskell JM, Jones AC, Chalker PR, Werner M, Aspinall HC, Taylor S, Taechakumput P, Heys PN: *Chem Vap Deposition* 2007, **13**:684.
17. Boscke TS, Govindarajan S, Kirsch PD, Hung PY, Krug C, Lee BH, Heitmann J, Schroder U, Pant G, Gnade BE, Krautschneider WH: *Appl Phys Lett* 2007, **91**:072902.
18. Mueller W, Aichmayr G, Bergner W, Erben E, Hecht T, Kapteyn C, Kersch A, Kudelka S, Lau F, Luetzen J, Orth A, Nuetzel J, Schloesser T, Scholz A, Schroeder U, Sieck A, Spitzer A, Strasser M, Wang PF, Wege S, Weis R: *Tech Dig -Int Electron Devices Meet* 2005, **34**.
19. Fu Chung-Hao, Chang-Liao Kuei-Shu, Wang Tien-Ko, Tsai WF, Ai CF: *Microelectronic Engineering* 2010, **87**:2014.
20. Xiong Yuhua, Tu Hailing, Du Jun, Ji Mei, Zhang Xinqiang, Wang Lei: *Appl Phys Lett* 2010, **97**:012901.
21. Southwick GRichard, Reed Justin, Buu Christopher, Butler Ross, Bersuker Gennadi, Knowlton BWilliam: *IEEE Tran Device and Materials Reliability* 2010, **10**:201.
22. Kim Joo-Hyung, Ignatova AVELislava, Kücher Peter, Weisheit Martin, Zschech Ehrenfried: *Current Applied Physics* 2009, **9**:e104.
23. Martin Dominik, Grube Matthias, Weber MWalter, Rüstig Jürgen, Bierwagen Oliver, Geelhaar Lutz, Riechert Henning: *Appl Phys Lett* 2009, **95**:142906.
24. Jonscher AK: *Dielectric Relaxation in Solids* Chelsea Dielectric Press, London; 1983.
25. Havriliak S, Negami S: *Polymer* 1967, **8**:161.
26. Curie J: *Ann Chim Phys* 1889, **18**:203.
27. von Schweidler E: *Ann Phys* 1907, **24**:711.
28. Potter RJ, Chalker PR, Manning TD, Aspinall HC, Loo YF, Jones AC, Smith LM, Critchlow GW, Schumacher M: *Chem Vap Deposition* 2005, **11**:159.
29. Watanabe H, Ikarashi N, Ito F: *Appl Phys Lett* 2003, **83**:3546.
30. Cheng YC: *Prog Surf Sci* 1977, **8**:181, and references therein.
31. Deal BE, Sklar M, Grove AS, Snow EH: *J Electrochem Soc* 1967, **114**:266.
32. Synder KC, Fowler WB: *Phys Rev B* 1993, **48**:13238.
33. Warren WL, Vanheusden K, Schwank JR, Fleetwood DM, Winokur PS, Devine RAB: *Appl Phys Lett* 1996, **68**:2993.
34. Warren WL, Vanheusden K, Fleetwood DM, Schwank JR, Shaneyfelt MR, Winokur PS, Devine RAB: *IEEE Tran Nuclear Science* 1996, **43**:2617.
35. Houssa M, Afanas'ev VV, Stesmans A, Heys MM: *Appl Phys Lett* 2000, **77**:1885.
36. Zhang JF, Zhao CZ, Groeseneken G, Degraeve R, Ellis JN, Beech CD: *J Appl Phys* 2001, **90**:1911.
37. Zhao CZ, Zhang JF, Chang MH, Peaker AR, Hall S, Groeseneken G, Pantisano L, De Gendt S, Heys M: *J Appl Phys* 2008, **103**:014507.
38. Taechakumput P, Zhao CZ, Taylor S, Werner M, Chalker PR, Gaskell JM, Jones AC, Drobnis M: In "Origin of Frequency Dispersion in High-k Dielectrics", *Semiconductor Technology Conference (ISTC2008), Proceeding of the 7th International Conference on Semiconductor Technology* Edited by: Ming Yang 2008, 20-26, ISBN 978-988-17408-1-6.
39. Kohlrausch F: *Pogg Ann Phys* 1863, **119**:352.
40. Williams G, Watts DC: *Trans Faraday Soc* 1970, **66**:80.
41. Alvarez F, Alegria A, Colmenero J: *Phys Rev B* 1991, **44**:7306.
42. Bello A, Laredo E, Grimau M: *Phys Rev B* 1999, **60**:12764.
43. Bokov AA, Mahesh Kumar M, Xu Z, Ye Z-G: *Phys Rev B* 2001, **64**:224101.
44. Jonscher AK: *Universal Relaxation Law—A sequel to Dielectric Relaxation in Solids* Chelsea Dielectrics Press, London; 1996.
45. Dissado LA, Hill RM: *Nature* 1979, **279**:685.
46. Hunt A: *J Non-Crystalline Solids* 1995, **183**:109.
47. Waser R, Klee M: *Inter Ferro* 1992, **2**:257.
48. Scher H, Montroll EW: *Phys Rev B* 1975, **12**:2455.
49. Wolters SR, Van Der Schoot JJ: *J Appl Phys* 1985, **58**:831.
50. Reisinger H, Steinlesberger G, Jakschik S, Gutsche M, Hecht T, Leonhard M, Schroder U, Seidl H, Schumann D: *Tech Dig -Int Electron Devices Meet* 2001, **267**.
51. Yu H, Liu H, Hao H, Guo L, Jin C, Yu Z, Cao M: *Appl Phys Lett* 2007, **91**:222911.
52. Sivakumar N, Narayanasamy A, Chinnasamy CN, Jeyadevan B: *J Phys: Condens Matter* 2007, **19**:386201.

doi:10.1007/s11671-010-9782-z

Cite this article as: Zhao et al.: Dielectric Relaxation of La-Doped Zirconia Caused by Annealing Ambient. *Nanoscale Res Lett* 2011 **6**:48.